CHEMISTRY OF MATERIALS
Article

Chem. Mater. **2011,** *23,* 1039–1049 1039
DOI:10.1021/cm1032173

Disulfonated Poly(arylene ether sulfone) Random Copolymer Blends Tuned for Rapid Water Permeation via Cation Complexation with Poly(ethylene glycol) Oligomers

Chang Hyun Lee,[†] Desmond VanHouten,[†] Ozma Lane,[†] James E. McGrath,*[,†,‡] Jianbo Hou,[†,‡] Louis A. Madsen,[†,‡] Justin Spano,[‡] Sungsool Wi,[‡] Joseph Cook,[§] Wei Xie,[§] Hee Jeung Oh,[§] Geoffrey M. Geise,[§] and Benny D. Freeman[§]

[†]*Macromolecules and Interfaces Institute, and* [‡]*Department of Chemistry, Virginia Polytechnic Institute and State University, Blacksburg, Virginia 24061, United States, and* [§]*Department of Chemical Engineering, Center for Energy and Environmental Resources, University of Texas at Austin, Austin, Texas 78758, United States*

Received November 9, 2010. Revised Manuscript Received December 15, 2010

Here we present fundamental studies of a new blending strategy for enhancing water permeability in ionomeric reverse osmosis membrane materials. A random disulfonated poly(arylene ether sulfone) copolymer containing 20 mol percent hydrophilic units (BPS-20) in the potassium salt ($-SO_3K$) form was blended with hydroxyl-terminated poly(ethylene glycol) oligomers (PEG, M_n = 600−2 000) to increase the water permeability of BPS-20. Blending PEG with the copolymer resulted in pseudoimmobilization of the BPS-20 polymer chains because PEG complexes with cations in the sulfonated polymer matrix. Strong ion−dipole interactions between the potassium ions of the BPS-20 sulfonate groups ($-SO_3K$) and the PEG oxyethylene ($-CH_2CH_2O-$) groups were observed via NMR spectroscopy. These interactions are similar to those reported between crown ethers and free alkali metal systems. The PEG oligomers were compatible with the copolymer at 30 °C in an aqueous environment. Transparent and ductile BPS-20_PEG blend films exhibited a Fox−Flory-like glass transition temperature depression as the PEG volume fraction increased. This depression depended on both PEG chain length and concentration. Both ion−dipole interactions and high coordination of $-CH_2CH_2O-$ with $-SO_3K$ yielded a defined and interconnected hydrophilic channel structure. The water permeability and free volume of BPS-20_PEG blend films containing 5 or 10 wt % PEG increased relative to BPS-20. The blend films, however, exhibited reduced sodium chloride (NaCl) rejection compared to BPS-20. Addition of PEG did not significantly alter the material's dry- and hydrated-state mechanical properties. Unlike commercial state-of-the-art polyamide RO membranes, the blend materials do not degrade when exposed to aqueous chlorine (hypochlorite) at pH 4. This comprehensive suite of measurements provides understanding of the molecular and morphological features needed for rational design of next-generation, chlorine-tolerant water purification materials.

Introduction

The ability to efficiently and economically produce fresh water from brackish and seawater is critical to addressing the growing global water shortage.[1] Reverse osmosis (RO) processes can be used to effectively remove salts and large solutes, including bacteria, from natural water using membranes with high flux and high salt rejection characteristics.[2,3] Currently, interfacially polymerized aromatic polyamide (PA) thin film composite membranes are the state-of-the-art RO technology because they offer high water flux and salt rejection (>99%) over a wide pH range.[4] PA membranes, however, exhibit poor resistance to degradation by chlorine-based chemicals such as sodium hypochlorite, which is used to disinfect water.[5] As a result, RO membrane performance degrades when PA membranes are continuously exposed to even low concentrations of available chlorine.[5,6]

Disulfonated poly(arylene ether sulfone) copolymers, now being developed for desalination membrane applications, are more stable in chlorinated solution than commercial PA membranes.[7,8] This result may be due to the absence of amide bonds in the sulfonated polysulfone;

(1) Service, R. F. *Science* **2006**, *313*, 1088.
(2) Baker, R. W. *Membrane Technology and Applications*, 2nd ed.; John Wiely & Sons, Ltd.: Chichester, U.K., 2004.
(3) Geise, G. M.; Lee, H. S.; Miller, D. J.; Freeman, B. D.; McGrath, J. E.; Paul, D. R. *J. Polym. Sci., Part B* **2010**, *48*, 1685.
(4) Cadotte, J. E. Interfacially synthesized reverse osmosis membrane. U.S. Patent 4,277,344, July 7, 1981.
(5) Knoell, T. *Ultrapure Water* **2006**, *23*, 24.
(6) Petersen, R. J.; Codotte, J. E. *Handbook of Industrial Membrane Technology*; Porter, M.C., Ed.; Noyes Publications: Park Ridge, NJ, 1990; pp 307−388.
(7) Park, H. B.; Freeman, B. D.; Zhang, Z. B.; Sankir, M.; McGrath, J. E. *Angew. Chem., Int. Ed.* **2008**, *47*, 6019.
(8) Paul, M.; Park, H. B.; Freeman, B. D.; Roy, A.; McGrath, J. E.; Riffle, J. S. *Polymer* **2008**, *49*, 2243.

Published on Web 01/07/2011

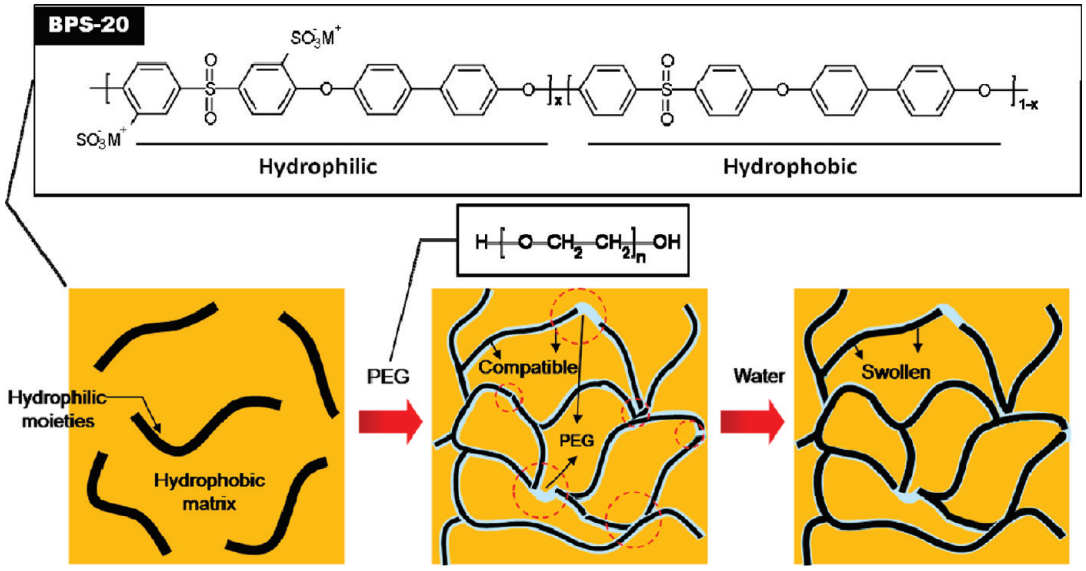

Figure 1. Pseudoimmobilization of PEG molecules with BPS-XX (M^+ = Na^+ or K^+, XX = degree of sulfonation in mol %). In BPS-20, x is 0.2.

amide bonds, such as those found in commercial PA RO membranes, are vulnerable to attack by chlorine-based chemicals.[9,10] Figure 1 presents the chemical structure of 20 mol % disulfonated poly(arylene ether sulfone) random copolymer (BPS-20). This copolymer, when studied as a cast film, exhibits stable RO performance, i.e., no substantial decrease in salt rejection or increase in water flux, after continuous exposure to chlorinated water at both high and low pH, i.e., >40 h at 500 ppm available chlorine.[7] A commercial PA membrane (SW30HR, Dow Film-Tec) experienced a 20% decrease in salt rejection within 20 h of exposure to the same chlorinated conditions.[7]

The water flux and salt rejection of BPS random copolymers exhibit a trade-off relationship;[3,11] highly water-permeable BPS materials tend to exhibit relatively low NaCl rejection and vice versa. BPS-20 has been identified as a candidate for desalination membrane applications because the NaCl rejection of BPS-20 is 99%. The BPS-20 water permeability (0.033 L μm m^{-2} h^{-1} bar^{-1}),[7] however, is low. To put this value in perspective, consider a scenario where the BPS-20 material has a 100 nm thick active layer in a composite membrane structure, similar to the accepted structure of commercially available state-of-the-art PA RO membranes. In this case, the water permeance would be expected to be 0.33 L m^{-2} h^{-1} bar^{-1} (2 000 ppm NaCl feed at 27.6 bar and pH 8).[7,12] This value can be compared to commercially available PA membranes such as DOW BW30 and SW30HR RO membranes whose water permeance is 3.3 L m^{-2} h^{-1} bar^{-1} (2 000 ppm NaCl feed at 15.5 bar and pH 8)[13] and 1.1 L m^{-2} h^{-1} bar^{-1} (32 000 ppm NaCl feed at 55.2 bar and pH 8),[14] respectively.[15]

This paper describes a new approach to increase the water permeability of BPS-20 and thus improve the material's desalination performance, via addition of poly(ethylene glycol) (PEG, Figure 1), a hydrophilic cation complexing agent. PEG oligomers were blended with BPS-20 to vary the resulting material's water permeability without changing the BPS material's degree of sulfonation. PEG systems have been widely used in self-assembly,[16,17] gas separation,[18] water purification,[19−23] and biomedical applications.[24,25] For example, PEG can be coated or grafted on ultrafiltration membranes to reduce fouling by oil−water mixtures[19] and to reduce blood coagulation in clinical hemodialysis.[21]

The water-soluble nature of PEG may limit its application to aqueous systems. PEG is often immiscible in many polymers because it does not interact favorably with many polymer matrixes. As a result, water often extracts PEG from blends with many polymers. To prevent such leaching, PEG chains can be immobilized via chemical modification (i.e., cross-linking[19] or grafting[20,21]) or hydrogen

(9) Brousse, C. L.; Chapurlat, R.; Quentin, J. P. *Desalination* **1976**, *18*, 137.
(10) Drzewinski, M.; Macknight, W. J. *J. Appl. Polym. Sci.* **1985**, *30*, 4753.
(11) Geise, G. M.; Park, H. B.; Sagle, A. C.; Freeman, B. D.; McGrath, J. E. J. Membr. Sci. **2010**, DOI: 10.1016/j.memsci.2010.11.054.
(12) Xie, W.; Cook, J.; Chen, C.; Park, H. B.; Freeman, B. D.; Lee, C. H.; McGrath, J. E. J. Membr. Sci. **2010**, submitted for publication.
(13) DOW. Water Solutions BW30-400 Product Specification, http://www.dow.com/liquidseps/prod/bw30_400.htm.
(14) DOW. Water Solutions SW30HR-380 Product Specification, http://www.dow.com/liquidseps/prod/sw30hr_380.htm.
(15) Van Wagner, E. M.; Sagle, A. C.; Sharma, M. M.; Freeman, B. D. *J. Membr. Sci.* **2009**, *345*, 97.
(16) Mao, G.; Castner, D. G.; Grainger, D. W. *Chem. Mater.* **1997**, *9*, 1741.
(17) Lee, M.; Jang, C. J.; Ryu, J. H. *J. Am. Chem. Soc.* **2004**, *126*, 8082.
(18) Chakrabarty, B.; Ghoshal, A. K.; Purkait, M. K. *J. Colloid Interface Sci.* **2008**, *320*, 245.
(19) Ju, H.; McCloskey, B. D.; Sagle, A. C.; Wu, Y. H.; Kusuma, V. A.; Freeman, B. D. *J. Membr. Sci.* **2008**, *307*, 260.
(20) Revanur, R.; McCloskey, B. D.; Breitenkamp, J.; Freeman, B. D.; Emrick, T. *Macromolecules* **2007**, *40*, 3624.
(21) Wang, P.; Tan, K. L.; Kang, E. T.; Neoh, K. G. *J. Mater. Chem.* **2001**, *11*, 783.
(22) Chou, W. L.; Yu, D. G.; Yang, M. C.; Jou, C. H. *Sep. Purif. Technol.* **2007**, *57*, 209.
(23) Chakrabarty, B.; Ghoshal, A. K.; Purkait, M. K. *J. Membr. Sci.* **2008**, *309*, 209.
(24) Van Alstine, J. M.; Malmsten, M. *Langmuir* **1997**, *13*, 4044.
(25) Lazzara, G.; Milioto, S. *J. Phys. Chem. B* **2008**, *112*, 11887.

bonding with acidic polymers (e.g., poly(acrylic acid)[26] and poly(methacrylic acid)[27]). There are, however, applications for PEG (i.e., pore forming agents)[22,23] where blending has been successfully employed.

PEG ether oxygen atoms form complexes with a variety of metal cations (Li^+, Na^+, K^+, Cs^+, and Rb^+) via ion−dipole interactions[28,29] similar to the behavior of cyclic ethers (e.g., crown ethers).[30−32] Such interactions in aqueous environments[33] have been suggested to explain the miscibility of PEG molecules and salt form sulfonated polymers, which are composed of sulfonate anions and metal cations ($-SO_3M$, where M is a cation of an alkali metal element such as Na or K). If PEG does complex with metal cations in sulfonated polymers, physical enthalpic interactions might effectively immobilize PEG in the sulfonated polymer matrix without the use of covalent bonds (pseudoimmobilization, Figure 1). These interactions could prevent PEG from leaching out of the polymer matrix upon exposure to water provided that the interactions are strong and sustained. Additionally, PEG may increase the water permeability of the sulfonated polymer matrix. This study seeks to understand the nature of the interaction between PEG and the disulfonated copolymer, BPS-20. The main objective is to systematically investigate the influence of PEG complexing agents, with different molecular weights and concentrations, on the physicochemical characteristics of the salt form of sulfonated polymer membranes. To probe these polymer blends, we employed pulsed-field gradient stimulated echo (PGSTE) NMR spectroscopy, which can track diffusion of water molecules in mixed matrixes over time using magnetic field gradients to label nuclear spins with NMR frequencies based on their locations.[34,35] Another major objective is to verify the efficacy of our pseudoimmobilization approach for forming fast water transport pathways for desalination applications. Finally, the chlorine resistance of the blend films was compared to a PA membrane.

Experimental Section

Materials. BPS-20 in the potassium salt form ($-SO_3K$) was synthesized by Akron Polymer Systems (Akron, OH) following published procedures.[36−40] The material used in this study, BPS-20 (the exact degree of sulfonation was 20.1 mol % measured using ^1H NMR) has an intrinsic viscosity of 0.82 dL g^{-1} in NMP with 0.05 M LiBr at 25 °C. PEG oligomers (molecular weight M_n = 600 (0.6k), 1 000 (1k), and 2 000 (2k) Da) with two −OH groups at their terminal ends (Figure 1) were purchased from Aldrich Chemical Co. and used as received. Dimethyl acetamide (DMAc) (Aldrich Chemical Co.) was used as a casting solvent without additional purification.

BPS-20_PEG Blends. After 2 g of BPS-20 was completely dissolved in DMAc at 30 °C, a PEG oligomer of the desired molecular weight was added to the BPS-20 solutions in two different concentrations, 5 wt % and 10 wt % where wt % was defined relative to the mass of BPS-20 in the solution. The resulting solutions were mixed for 1 day. Each solution (total solids concentration, 10 wt % in DMAc) was degassed under vacuum at 25 °C for at least 1 day and cast on a clean glass plate. Then, the cast solution was dried for 4 h at 90 °C and heated to 150 °C for 1 day under vacuum. The resulting films were easily peeled off of the glass plate and stored in deionized water at 30 °C for 2 days to further remove residual solvent. The nominal thickness of all films was approximately 30−40 μm, except those used for FT-IR measurement (20 μm). Transparent, ductile, and light-yellow BPS-20_PEG blend films were obtained. The yellow color increased with increasing PEG molecular weight and concentration. The BPS-20_PEG films are denoted as BPS-20_PEG molecular weight-PEG concentration (wt %). For instance, BPS-20_PEG0.6k-5 denotes a BPS-20 film containing 5 wt % of 0.6 kDa PEG.

Characterization. The thermal decomposition behavior of BPS-20_PEG films was investigated using a thermogravimetric analyzer (TGA) (TA Instruments Q500 TGA) operated at a heating rate of 10 °C min^{-1} from 50 to 600 °C in a 60 mL min^{-1} nitrogen sweep gas. Prior to the thermal decomposition measurements, all films were preheated in the TGA furnace at 110 °C for 15 min.

Transmission Fourier transform infrared (FT-IR) spectroscopy was used to study the interactions between BPS-20 and PEG. FT-IR spectra in the range of 4000−900 cm^{-1} were obtained using a Tensor 27 spectrometer (Bruker Optics).

Cross-polarization magic-angle spinning (CPMAS) ^{13}C NMR spectra were taken with a Bruker Avance II 300 MHz wide-bore spectrometer operating at Larmor frequencies of 75.47 MHz for ^{13}C and 300.13 MHz for ^1H nuclei. Thin film samples (50−60 mg) were cut into small pieces and packed into 4 mm magic angle spinning (MAS) rotors. Cross-polarization for 1 ms mixing time was achieved at 50 kHz rf-field at the ^{13}C channel with the ^1H rf field ramped linearly over a 25% range centered at 38 kHz. A pulse technique known as total suppression of spinning side bands (TOSS)[41] was combined with a CP sequence to obtain sideband-free ^{13}C MAS spectra at a 6 kHz spinning speed. The NMR signal averaging was achieved by coadding 2048 transients with a 4 s acquisition delay time. ^1H and ^{13}C $\pi/2$ pulse lengths were 4 and 5 μs, respectively. Small phase incremental alternation with 64 steps (SPINAL-64)[42] decoupling sequence at 63 kHz power was used for proton decoupling during ^{13}C signal detection.

(26) Nishi, S.; Kotaka, T. *Macromolecules* **1985**, *18*, 1519.
(27) Philippova, O. E.; Karibyants, N. S.; Starodubtzev, S. G. *Macromolecules* **1994**, *27*, 2398.
(28) Chan, K. W. S.; Cook, K. D. *Macromolecules* **1983**, *16*, 1736.
(29) Okada, T. *Macromolecules* **1990**, *23*, 4216.
(30) Pedersen, C. J. *J. Am. Chem. Soc.* **1967**, *89*, 2495.
(31) Gokel, G. W. *Crown Ethers and Cryptands*; Monographs in Supramolecular Chemistry; The Royal Society of Chemistry: Cambridge, U. K., 1991.
(32) Doan, K. E.; Heyen, B. J.; Ratner, M. A.; Shriver, D. F. *Chem. Mater.* **1990**, *2*, 539.
(33) Yanagida, S.; Takahasi, K.; Okahara, M. *Bull. Chem. Soc. Jpn.* **1977**, *50*, 1386.
(34) Li, J.; Wilmsmeyer, K. G.; Madsen, L. A. *Macromolecules* **2009**, *42*, 255.
(35) Stejskal, E. O.; Tanner, J. E. *J. Chem. Phys.* **1965**, *42*, 288.
(36) Wang, F.; Hickner, M.; Kim, Y. S.; Zawodzinski, T. A.; McGrath, J. E. *J. Membr. Sci.* **2002**, *197*, 231.
(37) Sumner, M. J.; Harrison, W. L.; Weyers, R. M.; Kim, Y. S.; McGrath, J. E.; Riffle, J. S.; Brink, A.; Brink, M. H. *J. Membr. Sci.* **2004**, *239*, 199.
(38) Kim, Y. S.; Dong, L.; Hickner, M. A.; Glass, T. E.; Webb, V.; McGrath, J. E. *Macromolecules* **2003**, *36*, 6281.
(39) Li, Y.; Wang, F.; Yang, J.; Liu, D.; Roy, A.; Case, S.; Lesko, J.; McGrath, J. E. *Polymer* **2006**, *47*, 4210.
(40) Li, Y.; VanHouten, R. A.; Brink, A. E.; McGrath, J. E. *Polymer* **2008**, *49*, 3014.
(41) Dixon, W. T. *J. Chem. Phys.* **1982**, *77*, 1800.
(42) Fung, B. M.; Khitrin, A. K.; Ermolaev, K. *J. Magn. Reson.* **2000**, *142*, 97.

To determine the glass transition temperature (T_g) of BPS-20 and BPS-20_PEG films, dynamic mechanical analysis (DMA) was conducted using a TA DMA 2980 (TA Instruments) in multifrequency tension mode; the temperature range was 0 to 300 °C with a ramp of 5 °C min^{-1} in a nitrogen atmosphere. The film samples were 4 mm in width, and each was subjected to a preload force of 0.025 N with an amplitude of 25 μm at a frequency of 1 Hz.

Water uptake (%) was calculated using the following equation:

$$\text{water uptake } [\%] = \frac{W_w - W_d}{W_d} \times 100$$

where W_d and W_w are the measured masses of dry and fully hydrated film samples, respectively. Each sample, approximately 5 × 5 cm^2, was dried in a vacuum oven at 110 °C for 1 day before measuring W_d and immersed in deionized water at 25 °C for 1 day before measuring W_w.

Surface morphologies were examined via tapping mode atomic force microscopy (AFM), using a Digital Instruments MultiMode scanning probe microscope with a NanoScope Iva controller. A silicon probe (Veeco, end radius < 10 nm, with a force constant = 5 N m^{-1}) was used to image the samples, and the set-point ratio was 0.82. Prior to measurement, all samples were equilibrated at 30 °C and 40% relative humidity (RH) for at least 12 h.

For pulsed-field gradient NMR spectroscopy, each film was cut into 5.5 × 5 mm^2 pieces and stacked together to a total mass of about 40 mg in a custom-built Teflon cell that was sealed to maintain water content during diffusion measurements. The test cell was loaded into a Bruker Avance III WB 400 MHz NMR spectrometer equipped with both a Micro5 triple-axis-gradient (maximum 300 G cm^{-1}) microimaging probe and an 8 mm double resonance ($^1H/^2H$) rf coil. The pulsed-gradient stimulated echo pulse sequence (PGSTE) was applied with a $\pi/2$ pulse time of 32 μs, a gradient pulse duration (δ) ranging from 1 to 3 ms, and diffusion time (Δ) ranging from 20 to 800 ms.[34] Each measurement was repeated with 32 gradient steps, and the maximum gradient strength was chosen to achieve 70−90% NMR signal attenuation.

The water permeability (P_w, L μm m^{-2} h^{-1} bar^{-1}) of BPS-20 and BPS-20_PEG films was evaluated at 25 °C using a dead-end cell apparatus with a feed of 2 000 ppm NaCl in deionized water. P_w was defined as the volume of water (V) permeated per unit time (t) through a membrane sample of area (A) and thickness (l) at a pressure difference (ΔP = 400 psig or 27.6 bar):

$$P_w = \frac{Vl}{At\Delta P}$$

Salt rejection (R, %) was measured using a dead-end cell filtration apparatus with an aqueous feed solution containing 2 000 ppm NaCl at pH 6.5−7.5 and a pressure of 400 psig. Salt rejection (R) was calculated as follows:

$$R = \frac{C_f - C_p}{C_f} \times 100$$

Here, C_f and C_p are the NaCl concentrations in the feed and permeate, respectively. Salt concentration was measured with a NIST-traceable expanded digital conductivity meter (Oakton Con 110 conductivity and TDS meter).

Tensile properties of the films were determined using an Instron 5500R universal testing machine equipped with a 200 lb load cell at 30 °C and 44−54% RH. Crosshead displacement speed and gauge length were set to 5 mm min^{-1} and 25 mm, respectively. Dogbone specimens (50 mm long and at least 4 mm wide) were cut from a single film. Prior to the measurement, each specimen was dried under vacuum at 110 °C for at least 12 h and then equilibrated at 30 °C and 4% RH. At least 5 measurements were collected, and the average of these measurements is reported.

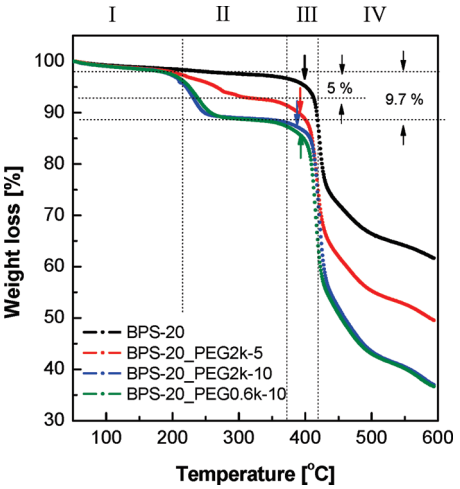

Figure 2. TGA thermograms of BPS-20 and BPS-20_PEG materials after soaking in deionized water at 30 °C for 150 days.

Results and Discussion

Because PEG is water-soluble and these materials are being evaluated for desalination applications, the stability of the hydrated films was explored. To determine whether PEG leached from the blend films, samples were stored in 30 °C deionized water for 150 days. After the 150 day soaking period, PEG content in the blend films was investigated using TGA, FT-IR, and NMR spectroscopy.

Figure 2 presents dynamic TGA thermograms of BPS-20 and BPS-20_PEG films. All of the materials exhibit three distinct thermal decomposition steps: (I) thermal evaporation of water molecules [< ~215 °C], (III) thermal desulfonation of BPS-20 [375−420 °C], and (IV) thermo-oxidation of BPS-20 [> ~420 °C].[36,43] The initial weight loss was ascribed to desorption of water from the samples; this weight loss increased with PEG concentration suggesting that water hydrates both the PEG molecules and BPS-20 sulfonate groups.

An additional thermal decomposition step (II), which is ascribed to thermo-oxidation of PEG [215−375 °C], was observed for the BPS-20_PEG blend samples. Thermal decomposition of PEG began around 215 °C; this temperature is higher than the initial thermal decomposition temperature (T_d) of pure PEG (~175 °C)[44] and similar to T_d of the ester bridge grafted PEG.[45] This increase in the initial decomposition temperature suggests that PEG

(43) Lee, C. H.; Park, H. B.; Chung, Y. S.; Lee, Y. M.; Freeman, B. D. *Macromolecules* **2006**, *39*, 755.
(44) Hechavarria, L.; Mendoza, N.; Altuzer, P.; Hu, H. *J. Solid State Electrochem.* **2010**, *14*, 323.
(45) Cappelli, A.; Galeazzi, S.; Giuliani, G.; Anzini, M.; Grassi, M.; Lapasin, R.; Grassi, G.; Farra, R.; Depas, B.; Aggravi, M.; Donati, A.; Zetta, L.; Boccia, A. C.; Bertini, F.; Samperi, F.; Vomero, S. *Macromolecules* **2009**, *42*, 2368.

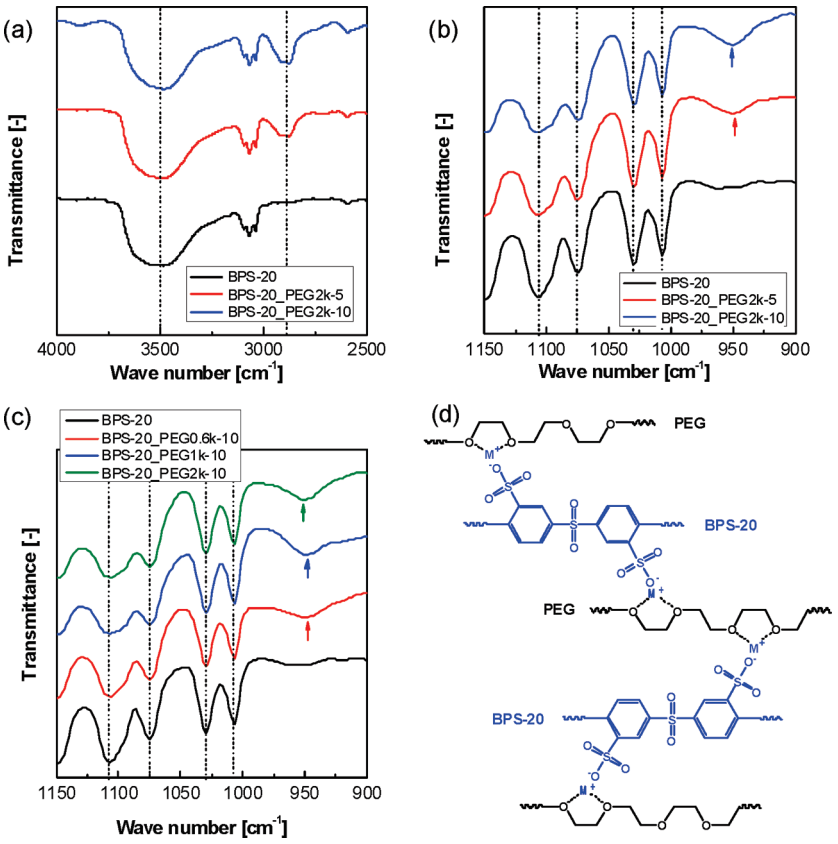

Figure 3. FT-IR spectra of BPS-20 and BPS-20_PEG materials with different concentrations (a and b) and molecular weights (c) of PEG. (d) Simulated cation binding with PEG molecules ($M^+ = Na^+$, K^+, and other metal cations).

interacts with BPS-20. Interactions of this nature may have bond energies similar to a weak covalent bond,[45] e.g., ester bond. PEG decomposition was quantified and compared to the amount of PEG initially added to the BPS-20 polymer matrix. The mass of PEG that remained in the blend matrix after the water soaking step was essentially equal to the mass of PEG that was initially present in the blend. Therefore, PEG did not leach from the blend matrix under our test conditions. We believe that the physical interaction between PEG and BPS-20 may arise from two sources: bonding interaction between the BPS-20 sulfonate groups and PEG −OH groups and ion−dipole interactions between PEG and the metal cation (K^+) associated with the BPS-20 sulfonate groups. The maximum BPS-20 thermal desulfonation temperature (T_{ds} ~398 °C) decreases by 5−12 °C upon addition of PEG. The reduction of T_{ds} was more significant for the BPS-20_PEG blends containing higher molecular weight PEG and higher PEG concentration.

Figure 3 presents FT-IR spectra of BPS-20 and BPS-20_PEG samples over the relevant range of vibration frequencies to confirm the identity of the interactions between PEG and BPS-20. To ensure that peak intensities were normalized, dry films of equivalent thicknesses (20 μm) were analyzed. The strong band at 2850 cm^{-1} in Figure 3a is assigned to the stretching vibration of the aliphatic alkyl ($-CH_2-$) PEG groups. The peak intensity of the $-CH_2-$ groups increased with PEG concentration, but the peak position did not shift. The bands at 1075 and 1030 cm^{-1} in Figure 3b are attributed to the symmetric stretching vibration of SO_3^- in BPS-20. The absorption band at 1107 cm^{-1} is associated with the $-SO_3K$ asymmetric stretching vibration. Its frequency is higher than the frequency (1098 cm^{-1}) of the corresponding vibration for the $-SO_3Na$ form of the same BPS-20 polymer. The observed frequency difference between the sodium and potassium form of the BPS-20 material may be due to the polarization difference between the ionic bonds in the $-SO_3K$ group and the $-SO_3Na$ group.[46] After addition of PEG, most of the peaks, including a stretching vibration band of diphenyl ether (−O−) at 1006 cm^{-1}, did not shift. This result indicates that hydrogen bonding between BPS-20 and PEG is not significant when the sample is in the dry state. In this discussion, the relative intensity changes in the SO_3^- bands were excluded because of the presence of a strong characteristic PEG band occurring between 1020 and 1200 cm^{-1}.[47]

In contrast, the absorption band (~950 cm^{-1}) in Figure 3b, assigned to the PEG aliphatic ether (−C−O−C−), became more distinct and shifted to higher frequency as PEG concentration increased. An analogous band shift was observed in BPS-20_PEG samples containing high molecular weight PEG (Figure 3c). The peak's shift suggests that a chemical species exists in the vicinity of

(46) Zundel, G. *Hydration and Intermolecular Interaction*; Academic Press: New York, 1969.
(47) Kim, C. H.; Kim, D. W.; Cho, K. Y. *Polym. Bull.* **2009**, *63*, 91.

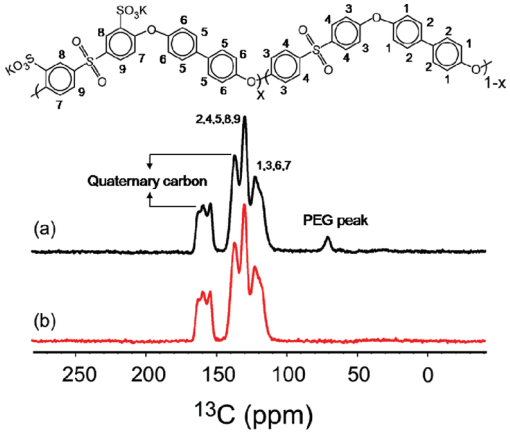

Figure 4. Solid state ^{13}C NMR spectra of (a) BPS-20_PEG0.6k-5 and (b) BPS-20.

the PEG molecules and physically interacts with the PEG aliphatic ether groups.

Free alkali metal cations, such as Na^+ and K^+, form complexes with PEG $-CH_2CH_2O-$ groups in both aqueous and nonaqueous solvents.[28,29,48,49] Furthermore, the ion−dipole interaction of PEG with the free metal cations is strengthened when long PEG chains (> 9 repeat units) are used.[28] In particular, the selectivity of long PEG chains to K^+ ions are promoted to the equivalent level of crown ethers (e.g., 18-crown-6).[33] PEG (> 14 units of $-CH_2CH_2O-$) used in this study may interact strongly with the K^+ ions that are associated with the BPS-20 $-SO_3^-$ groups (Figure 3d) because the ionic bond strength of the potassium sulfonate groups is theoretically stronger than the ion−dipole interaction between PEG and the sulfonate group metal cations[50] and the PEG $-CH_2CH_2O-$ groups have higher K^+ coordination numbers (6−7) compared to Na^+ (2−4).[29,51]

Solid state ^{13}C NMR spectroscopy of BPS-20_PEG, Figure 4, provided information about the interaction of BPS-20 and PEG. The solid state ^{13}C NMR used here was sensitive enough to monitor infinitesimal changes in the environment of the fully hydrated polymer system. Characteristic peaks for hydrated BPS-20 were consistently observed at the same chemical shifts regardless of PEG addition. Therefore, hydrogen bonding is not significant in hydrated BPS-20, and the ion−dipole interaction governs the macroscopic properties of both the dry and hydrated BPS-20_PEG system.

We believe that the ability of PEG to complex with metal cations affected the BPS-20_PEG glass transition temperature (T_g). Generally, the T_g of sulfonated polymers increases as the degree of sulfonation increases due to the bulky and ionic nature of the sulfonate groups.[52] For example, the BPS-20 T_g (270 °C, Figure 5) is higher

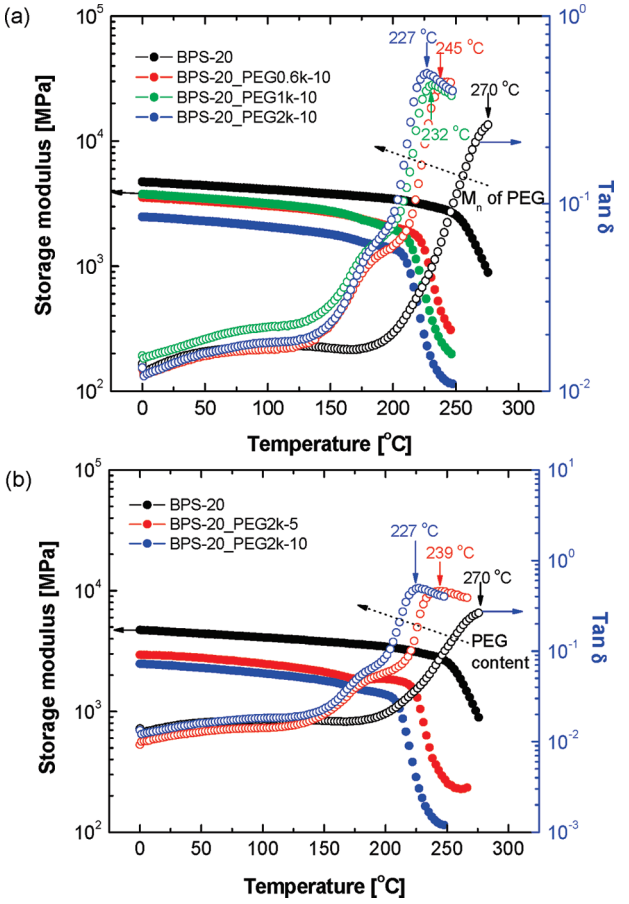

Figure 5. DMA profiles of BPS-20_PEG membranes with different (a) molecular weights and (b) concentration of PEG.

than that of BPS-00 (Radel, T_g = 220 °C).[53] Also, BPS-20 displays a broad T_g range, since the sulfonate groups are randomly distributed and may form ionic domains of different sizes within the hydrophobic matrix. When incorporated in BPS-20, PEG may disrupt the inter- and/or intramolecular ionic interactions between the sulfonate groups in the BPS-20 ionic domains (entropic effect); a decrease in T_g could indicate this disruption. A broad tan δ peak between 150 and 200 °C was observed using DMA. This broad peak can be attributed to sulfonated ionic domain dilution that occurs when PEG is introduced to BPS-20. Glass transition temperature depression behavior was especially significant in BPS-20_PEG samples containing long PEG chains and higher, i.e., 10 wt %, PEG concentration. For example, the T_g of BPS-20_PEG2k-10 dropped by 43 °C, comparable to the T_g of nonsulfonated BPS-00. The T_g of BPS-20_PEG samples decreased linearly with a slope that depended on PEG molecular weight (Figure S1 in the Supporting Information), which makes it possible to estimate the theoretical T_g change in BPS-20 upon PEG addition.

BPS-20_PEG samples are binary systems composed of BPS-20 and PEG (T_g = ∼−60 °C). The PEG homopolymer T_g is effectively constant over the molecular weights

(48) Izatt, R. M.; Pawlak, K.; Bradshaw, J. S.; Bruening, R. L. *Chem. Rev.* **1991**, *91*, 1721.
(49) Izatt, R. M.; Bradshaw, J. S.; Nielsen, S. A.; Lamb, J. D.; Christensen, J. J.; Sen, D. *Chem. Rev.* **1985**, *85*, 271.
(50) Kerres, J. A. *Fuel Cells* **2005**, *5*, 230.
(51) Besner, S.; Vallee, A.; Bouchard, G.; Prud'homme, J. *Macromolecules* **1992**, *25*, 6480.
(52) Xu, K.; Li, K.; Khanchaitit, P.; Wang, Q. *Chem. Mater.* **2007**, *19*, 5937.
(53) Solvay Advanced Polymers. www.Solvayadvancedpolymers.com.
(54) Back, D. M.; Schmitt, R. L. Ethylene Oxide Polymers. In *Kirk-Othmer Encyclopedia of Chemical Technology*; John Wiley & Sons: New York, 2004; Vol. *10*, pp 673−696.

chosen for this study (0.6k, 1k, and 2k).[54,55] Unlike immiscible systems that show distinct and constant glass transition temperatures for each component, the T_g of the BPS-20_PEG binary system depended on PEG concentration. The measured glass transition temperatures of BPS-20_PEG samples are very similar to theoretical predictions (202−232 °C) made using the Flory−Fox equation.[56] This comparison is commonly used to determine whether binary systems are miscible, compatible, or not at all miscible. In the following equation, $T_{g,i}$ and W_i represent the T_g and weight fraction of component i, respectively,

$$\frac{1}{T_{g,\,\text{BPS-20}_\text{P}\text{EG}}} = \frac{W_{\text{BPS-20}}}{T_{g,\,\text{BPS-20}}} + \frac{W_{\text{PEG}}}{T_{g,\,\text{PEG}}}$$

On the basis of the agreement between the measured BPS-20_PEG glass transition temperature data and predictions made using the Flory−Fox equation, we conclude that BPS-20 and PEG form a compatible system as a result of ion−dipole interactions between PEG and the BPS-20 sulfonate groups.

As the degree of sulfonation increases, the density of the BPS copolymer increases relative to unsulfonated BPS-00 (1.30 g cm^{-3}).[53] When PEG is incorporated into BPS-20, the density of the blend material decreases, as shown in Figure 6a. This decrease in density occurs because PEG acts as a plasticizer that increases BPS-20 chain spacing and free volume. The BPS-20_PEG density, when compared to the blend density calculated by assuming volume additivity (see Figure 6a), suggests that blending PEG with BPS-20 results in free volume changes that extend beyond what would be expected from simple mixing. Dry BPS-20_PEG samples exhibit higher densities than wet samples. Density measurements also suggest that the free volume of BPS-20_PEG increased as PEG chains became longer and more concentrated.

The water uptake of BPS-20_PEG (Figure 6b) correlated inversely with density. Water uptake increased as hydrophilic PEG was incorporated into BPS-20. Figure 6 indicates that low density BPS-20_PEG samples (i.e., high free volume samples) showed greater water uptake than samples of higher density (i.e., low free volume samples). Free volume is expected to influence water and salt transport properties in these polymers.[58]

In addition to water uptake, the surface morphology of sulfonated polymers can influence water permeability. AFM images, shown in Figure 7, indicate that the strong ion−dipole interaction of PEG with K^+ ions in BPS-20 sulfonate groups can induce a hydrophilic−hydrophobic nanophase separation even though BPS-20 is a random copolymer. In BPS-20 (Figure 7a), hydrophilic rod-like structures (darker regions) with average diameters of 9−12 nm are randomly distributed, yet connected,

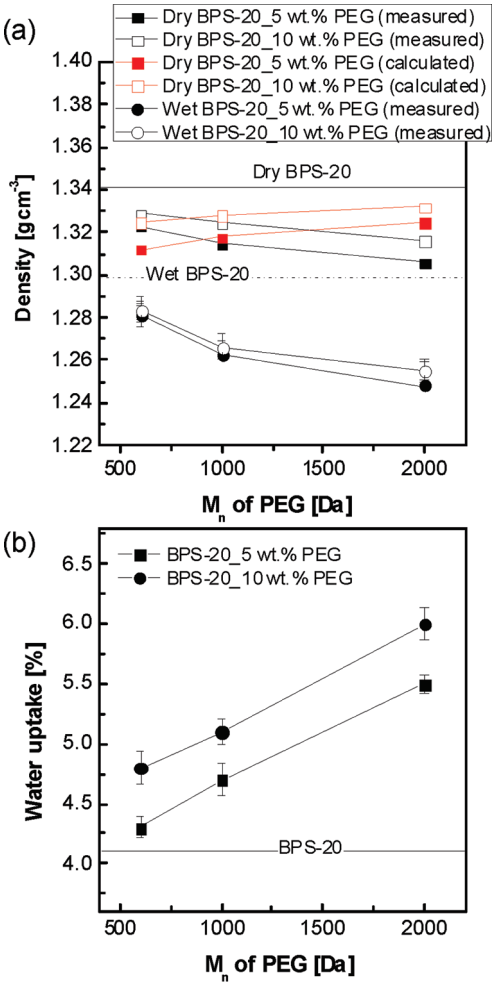

Figure 6. (a) Density and (b) water uptake of BPS-20_PEG. Calculated density of BPS-20_PEG was obtained from volume additivity: $1/\rho_{\text{BPS-20\_PEG}} = \varphi_{\text{BPS-20}}/\rho_{\text{BPS-20}} + \varphi_{\text{PEG}}/\rho_{\text{PEG}}$. Here, ρ and φ are the density and volume fractions, respectively, of each component in the blend. ρ_{PEG} was obtained from ref 57.

throughout the hydrophobic copolymer matrix (lighter regions).[36] When PEG was added to BPS-20, the morphology of the matrix changed. In BPS-20_PEG2k-5 (Figure 7b), the hydrophilic ionic domain size decreased to an average diameter to 3−6 nm and hydrophilic phase connectivity appeared to improve. This result may be related to strong ion−dipole interactions and the high coordination number of PEG $-CH_2CH_2O-$ units to K^+ ions in the BPS-20 sulfonate groups.[27,51] PEG (>9 units of $-CH_2CH_2O-$) typically prefers a meander conformation (e.g., helical coil structure) when exposed to free alkali metal cations.[28] The observed hydrophilic−hydrophobic phase separation depends on both PEG chain length and concentration. As PEG chain length increased, at a constant concentration (10 wt %, Figure 7c−e), the hydrophilic domains became more interconnected but generally decreased in size. Another morphological change was observed as the PEG concentration in BPS-20_PEG2k was varied from 5 to 10 wt % (Figure 7b,e). Unlike BPS-20_PEG2k-5, BPS-20_PEG2k-10 appears to have two different kinds of ionic domains: irregularly distributed ionic domains, with sizes similar to

(55) Read, B. E. Mechanical Relaxation in Some Oxide Polymers. *Polymer* **1962**, *3*, 529–542.
(56) Fox, T. G. *Bull. Am. Phys. Soc.* **1956**, *1*, 123.
(57) Zoller, P.; Walsh, D. J. *Standard Pressure-Volume-Temperature Data for Polymers*; Technomic Publishing Co., Inc.: Lancaster, PA, 1995.
(58) Yasuda, H.; Lamaze, C. E.; Ikenberry, L. D. *Die Makromol. Chem.* **1968**, *118*, 19.

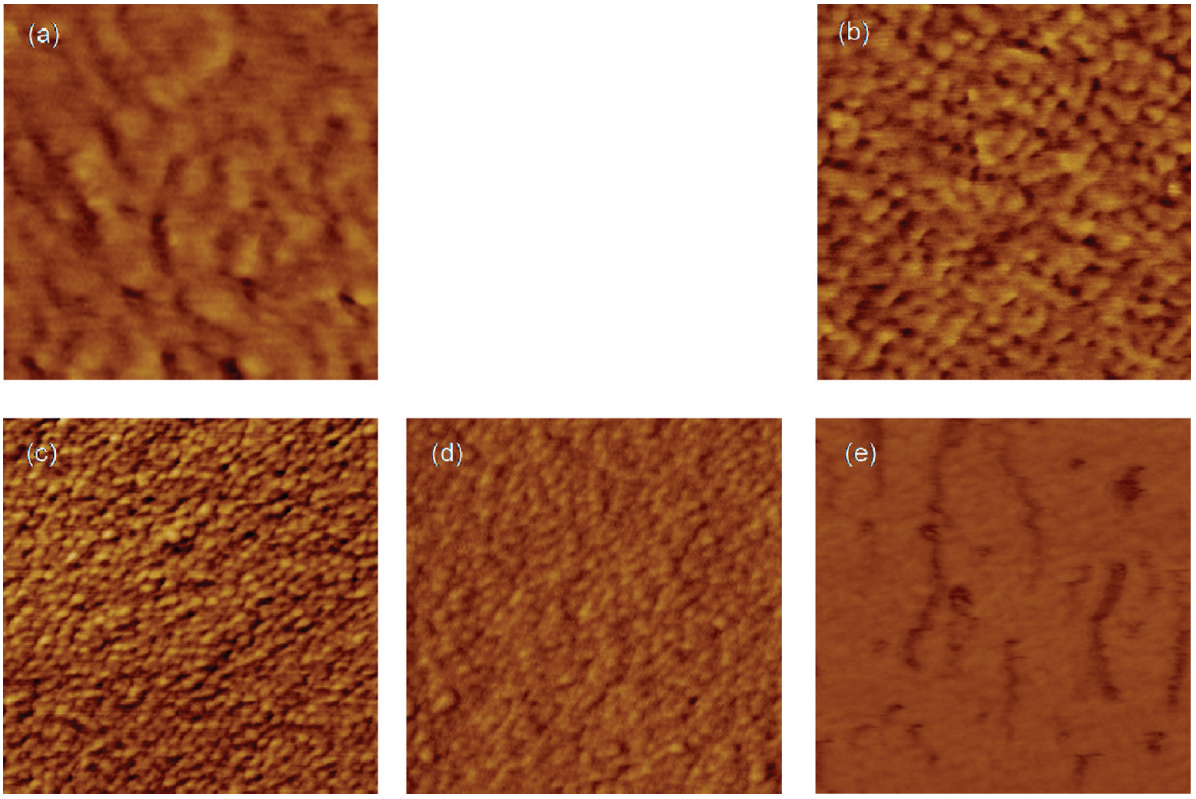

Figure 7. AFM images of (a) BPS-20, (b) BPS-20_PEG2k-5, (c) BPS-20_PEG0.6k-10, (d) BPS-20_PEG1k-10, and (e) BPS-20_PEG2k-10 materials in tapping mode. The dimensions of the images are 250 × 250 nm^2. The phase scale is 0−20°. The measurement was conducted at 35% RH.

BPS-20_PEG2k-5, and capillary-shape ionic domains, with sizes less than 1 nm. The ionic domains appear to be interconnected by long, tortuous hydrophilic pathways. The unevenly developed morphology may cause BPS-20_PEG2k-10 to have a lower water permeability than BPS-20_PEG2k-5.

PGSTE-NMR provides information about the diffusion of molecules in materials (i.e., the self-diffusion coefficient D of water in the polymer matrix). This technique is sensitive to the identity of the mobile species (e.g., water) and changes in sample environment, such as water content. D in a polymer matrix depends strongly on water uptake and temperature. Morphological changes also strongly influence the diffusion of water through the material. In fact, all samples exhibited reduced D values at long diffusion times (Δ), indicating the existence of tortuous hydrophilic pathways, similar to those observed in the AFM images of Figure 7. However, interpreting the water permeation behavior in these blend materials is not trivial since the PEG influences the hydrophilicity and ionic domain structure of the material. In this study, we used the Mitra equation[59] for porous media to assess diffusive restrictions (related to the surface-to-volume ratio of diffusion pathways, S/V) that result from the material's morphology.

$$D = D_0\left(1 - \frac{4}{9\sqrt{\pi}}\frac{S}{V}\sqrt{D_0\Delta}\right)$$

Here, S/V (meter^{-1}) is a factor associated with the internal roughness in the mixed matrix. An increase in S/V is expected to enhance water diffusion. By fitting D vs diffusion time (Δ), we extracted values for the effective "free" water diffusion coefficient D_0 (that expected at very small Δ) and S/V. Here, D_0 is interpreted as the effective intradomain diffusion coefficient of "free" water through the polymer's hydrophilic domain structure. Figure 8 shows the change in $D_0 \times S/V$ as a function of PEG molecular weight. $D_0 \times S/V$ values appear to correlate with water permeability data in Figure 9. This scaled water diffusion behavior in the mixed matrix materials decreased with increasing PEG chain length. However, the $D_0 \times S/V$ values for the BPS-20_PEG samples were greater than that for BPS-20. This finding indicates that S/V plays an important role in the diffusion and permeation of water through these samples.

Figure 9 presents water permeability and salt rejection data for BPS-20_PEG films. In the samples containing PEG, the water permeability of BPS-20_PEG increased relative to BPS-20. The increase in water permeability depended on both PEG concentration and chain length. Water permeability was greater in samples that contained a higher concentration of PEG; these samples, with 10 wt % PEG, also exhibited higher water uptake. Water permeability of BPS-20_PEG, however, decreased as PEG chain length increased. The water permeability of the BPS-20_PEG films is likely affected by the morphological changes that occur upon adding PEG, as indicated by AFM and scaled PGSTE-NMR (Mitra analysis[59]). We believe that the morphological contribution was

(59) Mitra, P. P. *Physica A* **1997**, *241*, 122.

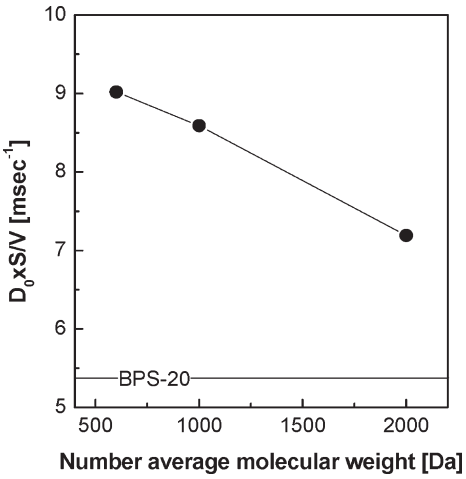

Figure 8. Diffusion behavior through tortuous water pathways in BPS-20_PEG 10% materials.

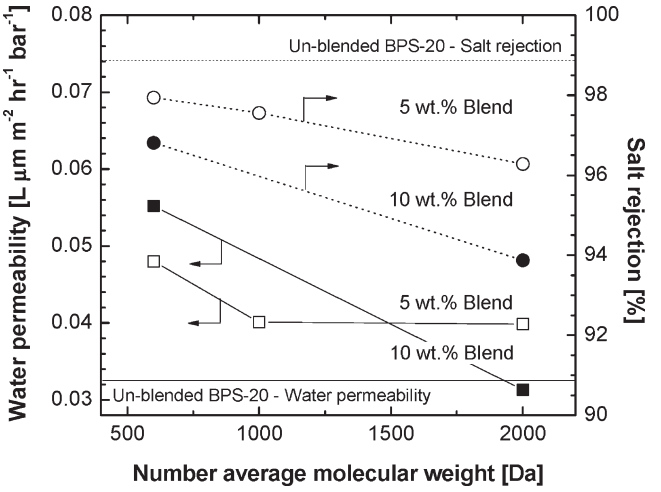

Figure 9. RO performance of BPS-20_PEG films: water permeability (left) and salt rejection (right).

particularly significant in BPS-20_PEG2k, which contained the highest PEG molecular weight. The long and tortuous channels in BPS-20_PEG2k-10 may restrict water diffusion and cause the water permeability to decrease even though the water uptake increased relative to that of BPS-20_PEG1k-10. Unlike other 10 wt % blends, the water permeability of BPS-20_PEG2k-10 was lower than BPS-20_PEG2k-5.

The water permeability of the blend materials may also be influenced by hydrogen bonding between water molecules and hydrophilic functional groups in the blend materials: BPS-20 sulfonate, PEG −OH, and PEG −O− groups. A constant amount of BPS-20 was used in BPS-20_PEG. Because the number of sulfonate groups was fixed, the difference in hydrogen bonding activity within different BPS-20_PEG samples is theoretically derived from the number of nonionic −OH and −O− PEG groups.[60] Table 1 shows the calculated number of the two functional groups per gram of BPS-20. The relative number of −OH groups increased as the PEG molecular weight decreased. Furthermore, the relative number of −OH groups increased when PEG concentration increased from 5 to 10 wt %. These results are similar to the water permeability results in Figure 9, suggesting the −OH groups may contribute more to water permeability than the −O− groups.

On the basis of the results shown in Figure 9, salt rejection decreases substantially with increases in PEG concentration and molecular weight. For example, in a BPS-20 sample prepared with 10 wt % of 2 kDa PEG, the rejection was 93.9%. For comparison, the rejection of pure BPS-20 was 98.9%. We speculate that the ion−dipole interaction between K^+ ions in the BPS-20 sulfonate groups and PEG oxyethylene units may weaken the electrostatic interaction of $-SO_3^-$ groups that would typically form physically cross-linked, ion-selective domains. Additionally, PEG incorporation into BPS-20 increases the material's water uptake. This increase in swelling reduces the concentration of sulfonate groups in the polymer matrix. This reduction in the sulfonate group concentration may result in decreased ion exclusion and, thus, decreased salt rejection.[3,61] Both the disruption of ion-selective domains and the dilution of sulfonate group concentration could result in reduced salt rejection as PEG concentration increases, which is consistent with the experimental observations. The reduced salt rejection was more significant in BPS-20_PEG samples prepared with higher molecular weight PEG. Longer PEG chains are associated with the formation of stronger ion−dipole interactions with K^+ ions in the BPS-20 sulfonate groups and highly water-swollen polymer matrixes.

Plasticizers increase the free volume of a polymer matrix and weaken the inter- and intramolecular interactions between the polymer chains; these effects often result in reduced mechanical properties. In the samples containing PEG, the stress and strain of BPS-20_PEG decreased (Figure S2 in the Supporting Information). The extent of this decrease, however, did not have a significant effect on the sample's toughness and ductility. Tensile modulus and strength were also unaffected by the amount of PEG used in this study (Table 1).

Resistance to degradation by chlorine-based disinfectants is critical for the long-term performance of RO membranes. An accelerated chlorine stability test was conducted by immersing each sample in a sealed vial containing a pH 4.0 ± 0.3 buffered aqueous solution of sodium hypochlorite (NaOCl) at concentrations of 100, 1 000, and 10 000 ppm.[62] Each material was immersed in the chlorinated solution for 2 time periods: 1 day and 1 week. Structural changes were monitored with solid state ^{13}C NMR spectroscopy (Figure 10). A reference PA film was obtained from the interfacial polymerization of *m*-phenylenediamine (3 wt % in water) and trimesoyl chloride (5 mM). The aromatic ring in the PA was vulnerable to

(60) Porter, M. R. *Handbook of Surfactants*, 2nd ed.; Blackie Academic and Professional, an imprint of Chapman & Hall: London, 1994.
(61) Helfferich, F. *Ion Exchange*; Dover Publications: New York, 1995.
(62) Jayarani, M. M.; Rajmohanan, P. R.; Kulkarni, S. S.; Kharul, U. K. *Desalination* **2000**, *130*, 1.

Table 1. Properties of BPS-20 and BPS-20_PEG Materials

	PEG functional groups per gram of BPS-20				mechanical properties [MPa]			
sample	−OH groups [equivalents/gram (BPS-20)]	relative ratio[a]	−O− groups [equivalents/gram (BPS-20)]	relative ratio[b]	tensile modulus	standard deviation	tensile strength	standard deviation
BPS-20					1 580	10	56	3
BPS-20_PEG0.6k-5	1.0×10^{20}	3.3	7.0×10^{20}	1.1	1 500	270	48	2
BPS-20_PEG0.6k-10	2.0×10^{20}	6.7	1.4×10^{21}	2.2	1 620	240	48	6
BPS-20_PEG1k-5	6.0×10^{19}	2.0	6.3×10^{20}	1.0	1 810	240	55	1
BPS-20_PEG1k-10	1.2×10^{20}	4.0	1.3×10^{21}	2.0	1 840	250	54	5
BPS-20_PEG2k-5	3.0×10^{19}	1.0	6.7×10^{20}	1.0	1 750	210	57	2
BPS-20_PEG2k-10	6.0×10^{19}	2.0	1.3×10^{21}	2.0	1 600	290	58	3

[a] Number of $[-OH]_{sample}$/number of $[-OH]_{BPS\text{-}20\_PEG2k\text{-}5}$. [b] Number of $[-O-]_{sample}$/number of $[-O-]_{BPS\text{-}20\_PEG2k\text{-}5}$

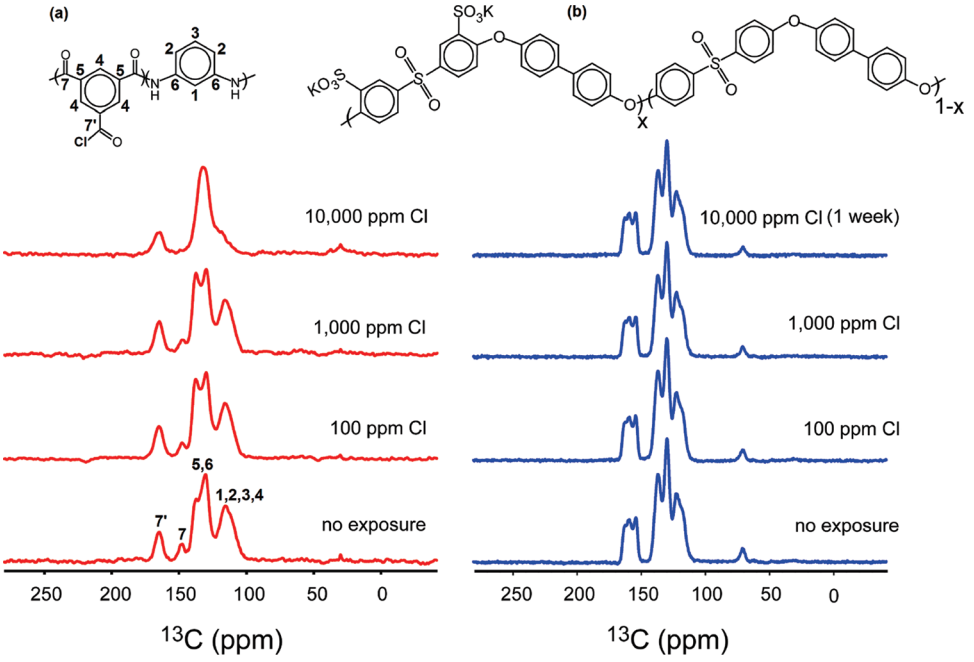

Figure 10. Solid state ^{13}C NMR spectra of (a) PA and (b) BPS-20_PEG0.6k-5 after exposure to different chlorine concentrations.[62].

electrophilic chlorine attack as reported in the literature.[63,64] The phenyl ring C−H peaks of the PA film decreased with exposure to chlorine due to the formation of C−Cl bonds (Figure 10a). Also, the intensity of the carbonyl carbon peak for the PA film decreased as PA chains were degraded by chlorine attack at the carbonyl sites. In contrast, none of the BPS-20 peaks showed changes in position or intensity after exposure at 10 000 ppm chlorine at pH 4.0 ± 0.3 for 1 week (Figure 10b). We note, however, that PEG concentration in the blend materials decreases as chlorine concentration or exposure time increases. For example, in BPS-20_PEG0.6k-5, the PEG content obtained from relative peak integration with respect to the BPS-20 peaks fell to about 60% of its initial value after 1 day of immersion in 1 000 ppm of chlorine. This may be related to oxidative degradation of PEG.[65] No additional PEG was lost when the films were exposed to highly concentrated solutions of chlorine for a long time. A similar trend was observed for BPS-20_PEG0.6k-10. This suggests that the ion−dipole interaction between PEG and BPS-20 is stable under harsh conditions, although exposure to chlorinated water may weaken the interaction.

Conclusions

Blends of PEG with BPS-20, a potassium salt form sulfonated random copolymer, gave rise to strong ion−dipole interactions between K^+ ions in the BPS-20 sulfonate groups and PEG. These interactions are similar to the behavior of crown ethers and alkali metal cations.[30−32] These interactions resulted in high compatibility between BPS-20 and PEG and prevented PEG from being extracted from the blends by exposure to water for long periods of time (pseudoimmobilization). The strength of the ion−dipole interaction was similar to a weak covalent bond, as shown in the thermal decomposition behavior of PEG in the blend materials. The cation complexing capability of PEG molecules weakened the inter- or

(63) March, J. *Advanced Organic Chemistry: Reactions, Mechanisms, and Structure*, 4th ed.; John Wiley: New York, 1992.
(64) Bieron, J. F.; Dinan, F. J. Rearrangement and elimination of the amide group. In *The Chemistry of Amides*; Zabicky, J., Ed.; Wiley Interscience: New York, 1970; pp 263−266.
(64) Bieron, J. F.; Dinan, F. J. Rearrangement and elimination of the amide group. In *The Chemistry of Amides*; Zabicky, J., Ed.; Wiley Interscience: New York, 1970; pp 263−266.
(65) Chen, S. F.; Zheng, J.; Li, L. Y.; Jiang, S. Y. *J. Am. Chem. Soc.* **2005**, *127*, 14473.

intramolecular hydrogen bonding between sulfonate groups, which typically form physically cross-linked ionic domains. Increases in PEG molecular weight and concentration resulted in a reduction of the blend's glass transition temperature. This plasticization led to increased free volume and increased water uptake. The ion−dipole interaction and the high coordination number of the PEG $-CH_2CH_2O-$ units to K^+ ion in the BPS-20 sulfonate groups converted the sample surface morphology from a random distribution of hydrophilic domains in the hydrophobic polymer matrix into a more defined hydrophilic−hydrophobic nanophase separated morphology. This trend was more pronounced in BPS-20_PEG samples containing high concentrations of PEG. Increased water uptake and interconnected hydrophilic domains, resulting from the addition of PEG, increased the water permeability of BPS-20_PEG compared to BPS-20. Long PEG chains formed long and tortuous hydrophilic channels that decreased water diffusion (D_0 S/V) and, thus, water permeation. Furthermore, NaCl rejection decreased upon the addition of PEG likely because of weakened electrostatic interactions between K^+ ions and $-SO_3^-$ groups and reduced ionic exclusion due to dilution of the BPS-20 sulfonate groups caused by increased water uptake. The decrease in NaCl rejection was minimized when short PEG chains (e.g., 0.6k) were used. With the addition of PEG, water permeability increased to about 200% compared to the unblended BPS-20 starting material. The influence of PEG addition on sample toughness and ductility was negligible. Unlike PA membranes, which degrade when exposed to chlorinated solutions, BPS-20_PEG resisted degradation by chlorine after prolonged exposure to high chlorine concentrations.

Incorporating PEG molecules into low disulfonated salt form random copolymers offers an effective and economical avenue to increase the material's water permeability and fouling resistance.[15,19] However, the BPS-20 polymer matrix and hydroxyl-terminated PEG blends may not exhibit the necessary water permeability and salt rejection to be an attractive RO membrane material. Therefore, our ongoing studies are focusing on random copolymers with higher degrees of sulfonation and ion-selective PEG. Finally, we will attempt to synthesize multiblock copolymers containing PEG moieties to improve the hydrophilic and hydrophobic phase-separation of these chemically stable materials.

Acknowledgment. This work was supported by Dow Water & Process Solutions. This work was also supported in part by the National Science Foundation (NSF)/Partnerships for Innovation (PFI) Program (Grant No. IIP-0917971). This material is based in part (L. A. Madsen, and J. Hou) upon work supported by the National Science Foundation under Award Number DMR 0844933.

Supporting Information Available: Glass transition temperature changes depending on PEG molecular weight and concentration and stress−strain (S−S) curves of BPS-20 and BPS-20_PEG materials (PDF). This material is available free of charge via the Internet at http://pubs.acs.org.